Available online at www.sciencedirect.com

SciVerse ScienceDirect

Ceramics International 39 (2013) 4151–4162

CERAMICS INTERNATIONAL

www.elsevier.com/locate/ceramint

Characterization of silicon carbide joints fabricated using SiC particulate-reinforced Ag–Cu–Ti alloys

M.C. Halbig[a], B.P. Coddington[b], R. Asthana[c,*], M. Singh[d]

[a]NASA Glenn Research Center, Cleveland, OH, USA
[b]University of Wisconsin-Madison, Madison, WI, USA
[c]University of Wisconsin-Stout, Menomonie, WI, USA
[d]Ohio Aerospace Institute, NASA Glenn Research Center, Cleveland, OH, USA

Received 9 September 2012; received in revised form 30 October 2012; accepted 31 October 2012
Available online 13 November 2012

Abstract

CVD silicon carbide was brazed to itself using two Ag–Cu–Ti braze alloys reinforced with SiC particulates to control braze thermal expansion and enhance joint strength. Powders of the braze alloys, Ticusil (composition in wt%: Ag–26.7Cu–4.5Ti, T_L: 900 °C) and Cusil-ABA (Ag–35.3Cu–1.75Ti, T_L: 815 °C) were pre-mixed with 5, 10 and 15 wt% SiC particulates (~20–30 μm) using glycerin to create braze pastes that were applied to the surfaces to be joined. Joints were vacuum brazed and examined using optical microscopy (OM), field emission scanning electron microscopy (FESEM), energy dispersive spectroscopy (EDS) and the Knoop hardness test. The SiC particles were randomly distributed in the braze matrix and bonded to it via reaction with the titanium from the braze alloy. Titanium together with Si and C segregated at the particle/braze interface, and promoted nucleation and precipitation of the Cu-rich secondary phase on particle surfaces. The Si–Ti–C-rich reaction layers also formed at the interface between CVD SiC substrate and the braze alloy. The loss of Ti in the reaction with SiC particulates did not impair either the bond quality or the thickness of the reaction layer on the CVD SiC substrate. Microhardness measurements showed that the dispersed SiC particulates lowered the braze hardness by depleting the braze matrix of Ti. Theoretical calculations indicated the CTE of the braze to decrease by nearly 45–60% with the incorporation of about 45 vol% SiC.

Keywords: Silicon carbide; Brazing; Particulate; Microhardness

1. Introduction

In monolithic form, silicon carbide ceramics are widely used in a variety of structural, functional and semiconducting applications. However, net-shape ceramic parts are expensive and difficult to fabricate. Therefore, robust joining and integration technology such as brazing attains importance in manufacturing. In addition, like most ceramics, SiC is seldom used in isolation and this requires it to be integrated to diverse materials including metals. For example, there is interest to develop a micro-electro–mechanical system lean direct (fuel) injector for advanced aircraft gas turbine engines [1,2] for which chemical vapor deposited silicon carbide (SiC) ceramics have to be joined together and also integrated with low-expansion alloys such as kovar [3]. There is thus a critical need to develop and demonstrate promising technology to join SiC to itself and to other materials, particularly metals.

Brazing is simple, cost-effective and proven technology to join ceramics. However, joining and integration technologies for advanced silicon carbide ceramics have not been widely investigated. Prior work on brazing of silicon carbide ceramics to themselves and to metals [3–8] has made use mainly of Ag–Cu–Ti brazes [3,6–8] although Co-base [9,10] and Ni-base [11] brazes also have been used. It has been reported [11] that Ni-base brazes form a Ni–Si liquid with the free silicon in the ceramic substrate, which reacts with the SiC to form deleterious low-melting point phases at the joined interface. Particulate-reinforced brazes also have been successfully used to join both SiC [11,12] and other ceramics [13,14] as well

*Corresponding author.
E-mail address: AsthanaR@uwstout.edu (R. Asthana).

0272-8842/$ - see front matter © 2012 Elsevier Ltd and Techna Group S.r.l. All rights reserved.
http://dx.doi.org/10.1016/j.ceramint.2012.10.271

as ceramic–matrix composites such as C/SiC [15–17]. SiC has attractive physical and mechanical properties and a moderate CTE ($4.1 \times 10^{-6}\,K^{-1}$) and reinforcing the braze matrix with SiC particulates (SiCp) would permit CTE control for residual stress management besides strengthening the matrix as in a composite. Knowles et al. [12] reported improvements in joint strength in monolithic SiC with 5% SiC (~5 μm) dispersed in Ag–Cu–Ti brazes to which excess Ti was added to compensate for its loss in reactions due to increased ceramic surface area. Improvements in joint strength have also been observed by Qin and Yu [17] who brazed C/C to Ti–6Al–4V using SiC particulate-reinforced Ag–Cu–Ti alloys, and by Blugan et al. [13] who joined Si_3N_4 to steel using a Ag–Cu–In–Ti braze reinforced with SiC. Besides particulate-reinforced brazes, short fiber-reinforced Ag–Cu–Ti brazes also have been observed to increase the joint strength of ceramic–matrix composites such as C/SiC [15,16]. Thus, there is considerable interest in using reinforced metallic brazes to join ceramics.

With reference to the use of Ag–Cu–Ti brazes reinforced with SiCp to join SiC substrates, only one study by Knowles et al. [12] could be found. In their study, these authors used 30 min brazing time to join SiC; presumably to promote interfacial reactions and bonding. In actual practice, shorter brazing times are generally used; therefore, studying the effect

Table 1
Composition and Selected Properties of Brazes Used.

Braze (composition, wt%)	T_L (°C)	T_S (°C)	*E* (GPa)	*YS* (MPa)	*UTS* (MPa)	*CTE* ($\times 10^{-6}C^{-1}$)	% *El.*	*K* (W/m K)
Cusil-ABA® (Ag–35.3Cu–1.75Ti)	815	780	83	271	346	18.5	42	180
Ticusil® (Ag–26.7Cu–4.5Ti)	900	780	85	292	339	18.5	28	219

E: Young's modulus, *YS*: yield strength, *UTS*: tensile strength, *CTE*: coefficient of thermal expansion, %*El*: percent elongation, *K*: thermal conductivity. Cusil-ABA® and Ticusil® are active braze alloys from Morgan Advanced Ceramics, Hayward, CA.

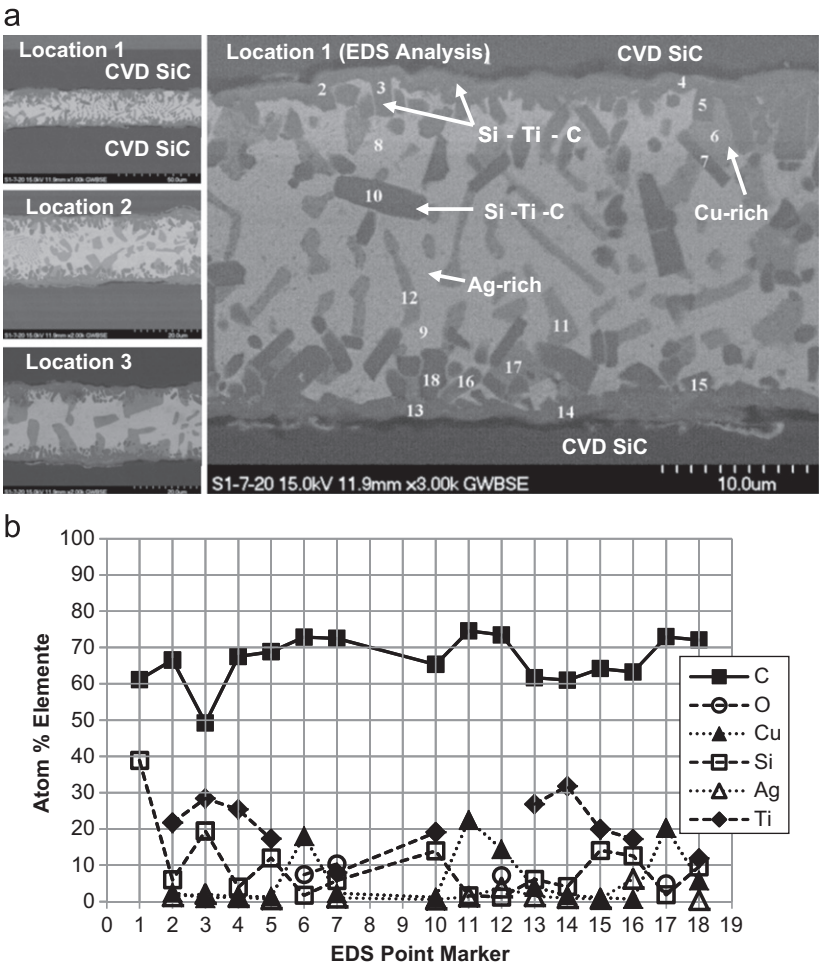

Fig. 1. (a) SEM backscattered electron (BSE) images of different locations of a CVD SiC/Ticusil/CVD SiC joint with 0 wt% SiC particulates, and a higher magnification view of the joint; (b) relative atomic percentages of the alloying elements at point markers in (a). The data at point markers 8 and 9 are not shown owing to a signal access error in EDS.

of short time contact on structure, composition and properties would be of interest. In addition, Knowles et al. [12] used fine SiC particles (1–7 μm) to reinforce the braze. With fine particles (small inter-particle spacing), constrained deformation of the ductile matrix will limit plastic flow thus contributing to the strength which was actually observed [12]. In contrast, with coarse particles, inter-particle spacing would increase thereby facilitating matrix deformation and contributing to toughness. Generally, fine particles improve the strength but degrade the fracture toughness. It must be recognized that failure can originate from particle cracking, interfacial debonding, or matrix cracking. Coarse particles increase the fracture tendency because of a larger defect population but decrease the interface area where debonding could occur. Because of elastic/plastic incompatibility at a metal/ceramic interface, CTE-mismatch induced residual stresses during cooling from the brazing temperature generate dislocations at the particle/braze interface that increase the modulus, yield strength, and fracture stress. Additional effects of particle size such as those from grain refinement may be possible. Although grain size of the braze matrix was not reported in Ref. [12], it is conceivable that fine particles with a large surface area will enhance nucleation, grain refinement and strengthening whereas fine particles with small inter-particle spacing will constrain second phase growth due to diffusion barrier effects. In addition, fine particles can lead to pronounced particle-to-particle contact, increased clustering tendency, and metal-starved regions even at moderate volume fractions. Because of the preceding known effects of particle size and to complement prior work [12] on fine SiC, it would be of interest to examine how coarse particles modulate the structure and properties of ceramic joints.

This research examines the effect of coarse SiC particles dispersed in two Ag–Cu–Ti active braze alloys, Cusil-ABA and Ticusil, on the structure, composition and microhardness of SiC-to-SiC joints created in 5 min brazing time. The initial goal was to study the effect of SiC particulates for SiC-to-SiC bonding to evaluate the trends with particulates. A future goal will be evaluating the effectiveness of SiC dispersion on SiC-to-metal bonding for advanced aircraft gas turbine engine applications such as lean direct (fuel) injector alluded to in the preceding discussion. The microstructure and composition of the joint interface, and the hardness characteristics of the joints with different percentages of SiC additions to the braze

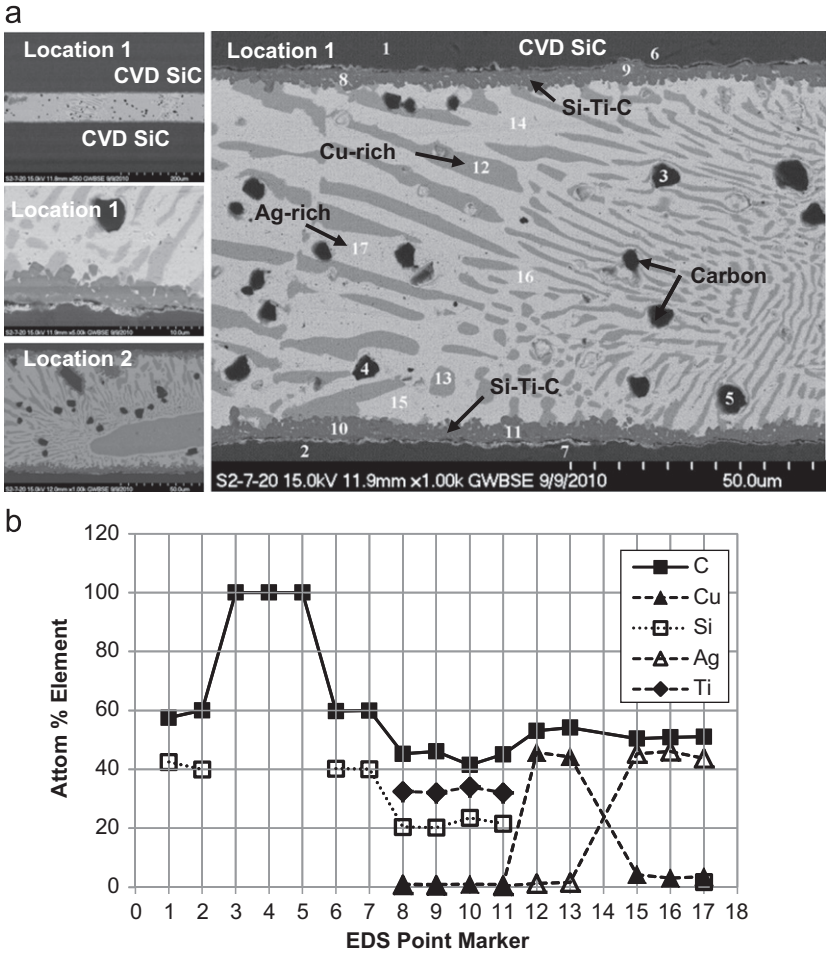

Fig. 2. (a) SEM BSE images of different locations of a CVD SiC/Ticusil/CVD SiC joint with 5 wt% SiC particulates, and a higher magnification view of the joint; (b) relative atomic percentages of the alloying elements at point markers in (a). Composition data at point marker 14 are not shown owing to a signal access error in EDS.

were evaluated using field emission scanning electron microscopy (FESEM), energy dispersive spectroscopy (EDS), and Knoop microhardness test.

2. Experimental procedure

Chemical vapor deposited (CVD) silicon carbide was used as the substrate material. The substrate was sliced into 2.54 cm × 1.25 cm × 0.25 cm pieces using a diamond saw and ultrasonically cleaned in acetone for 15 min prior to joining. Two commercial braze powders, Cusil-ABA and Ticusil, from Morgan Advanced Ceramics, Hayward, CA were used for joining. A limited number of brazing runs were made using Cusil-ABA and Ticusil in foil form. The composition and selected properties of the braze alloys are given in Table 1. No excess Ti was added to the braze matrix to compensate for its loss in interfacial reactions; this was done to characterize the behavior of unmodified braze matrix in the presence of SiCp.

Weighed quantities of braze powders and SiC particulates (nominal size ~20–30 μm) were manually mixed to yield 5, 10 and 15 wt% of SiCp. A few drops of glycerin were added to the powder mixture to make a thick paste with dough-like consistency. The paste was applied using a spatula to the surfaces to be joined. The assembly was loaded with a normal pressure of 0.2–0.4 MPa and heated in an atmosphere-controlled furnace to the brazing temperature (typically 15–20 °C above the braze liquidus) under vacuum (~10^{-6} to 10^{-5} Torr), isothermally held for 5 min at the brazing temperature, and slowly cooled to room temperature at a controlled rate (~5 °C per min to 500 °C, followed by furnace cooling). The joined samples were mounted in epoxy and polished in preparation for metallurgical examination. The joint region was examined using optical microscopy, field emission scanning electron microscopy (FESEM), and energy-dispersive spectroscopy (EDS). Hardness measurements across the joint interfaces were made using a Knoop microindenter on a Duramin-A 300 machine under a load of 200 g and loading time of 10 s.

3. Results and discussion

3.1. Microstructure of Ticusil joints

Fig. 1 shows the joint microstructure in CVD SiC joined to itself using unreinforced Ticusil braze. The braze

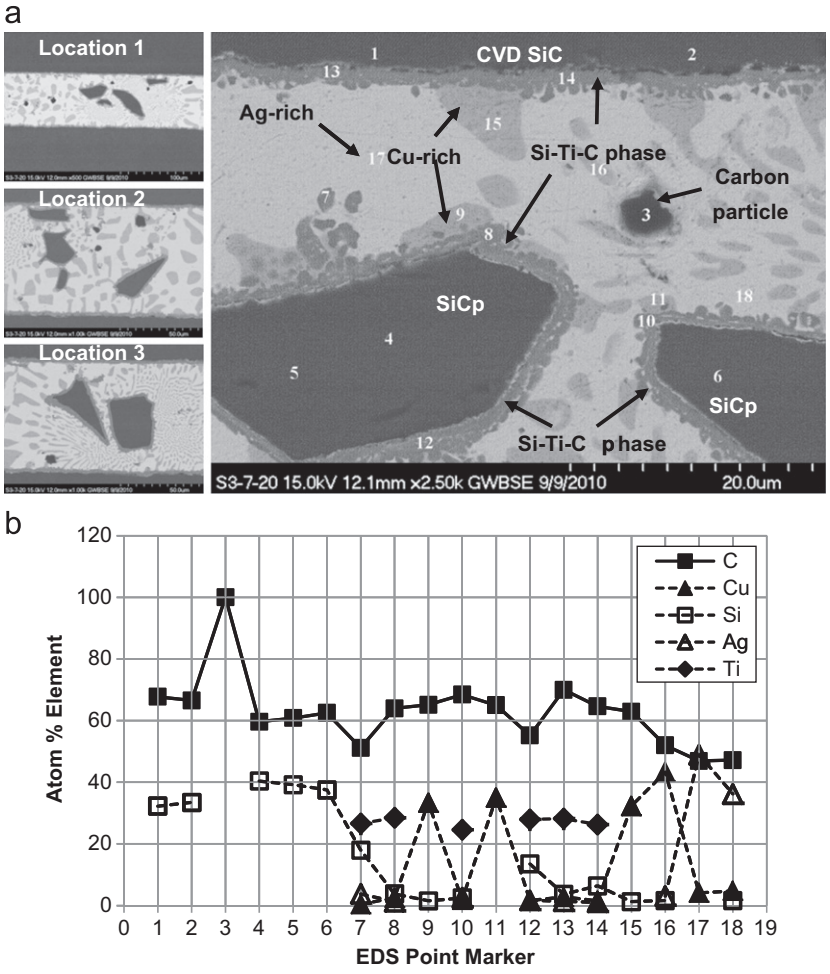

Fig. 3. (a) SEM BSE images of different locations of a CVD SiC/Ticusil/CVD SiC joint with 10 wt% SiC particulates, and a higher magnification view of the joint; (b) relative atomic percentages of the alloying elements at point markers in (a).

interlayers are well-defined and consistent and the joined SiC substrates reveal excellent, crack-free joints. The substrate/braze interface is enriched in Si, Ti and C (points 2, 4, 13 and 14, Fig. 1(b)) and the braze matrix shows the characteristic two-phase eutectic structure comprised of Cu-rich (points 6, 11, 12 and 17, Fig. 1(b)) and Ag-rich (Fig. 1(a)) phases. Additionally, large plate-like precipitates of a Si–Ti–C-rich phase (Fig. 1a) are also detected within the braze matrix. This points toward dissolution of SiC substrate in molten braze. The microstructure of the joint made using braze foil was similar to the microstructure of the joints made using paste. The introduction of 5 wt% SiC (13 vol% SiC) led to chemical interaction between the braze matrix and both SiCp and CVD SiC substrates (Fig. 2a shows a region where carbon particles abound; other views and locations show SiCp). There is evidence of the presence of nearly pure carbon particles (points 3, 4 and 5, Fig. 2a & b) in the braze that are bonded to Ticusil (the starting SiC powders may have contained some carbon particles as an impurity with SiCp). Both the CVD substrate/braze interface (points 8–11, Fig. 2(a)) and the SiCp/braze interface (not visible in Fig. 2(a)) were observed to be enriched in Ti, Si and C. Thus, besides the major Ag-rich (points 15–17, Fig. 2(a)) and Cu-rich (points 12 and 13, Fig. 2(a)) phases of the braze matrix, the SiC/SiC joint of Fig. 2 also contains SiCp, carbon(p), and reaction layers enriched in Ti, Si and C at interfaces between the CVD SiC and Ticusil, and between SiCp and Ticusil.

With 10 wt% SiC (25 vol% SiC, Fig. 3) and with 15 wt% SiC (43 vol% SiC, Fig. 4) added to Ticusil, there is no change in the composition of the reaction layer which is enriched in Ti, Si, and C as before, indicating likely formation of titanium carbides and titanium silicides. Although interfacial reaction layers such as those shown in Figs. 3 and 4 appear to be comprised of a homogeneous single phase, our recent TEM interface characterization studies [18–20] on brazed joints of SiC [18] and other ceramics [19,20] have shown that such reaction layers have a complex structure and usually contain multiple phase constituents.

A copper-rich secondary phase (Figs. 3a and 4a) has precipitated on the reaction layer on SiCp and SiC substrate surface. The precipitation of Cu-rich phase at the interface can be understood with reference to the contact angle of Cu on titanium carbide [21]. Copper

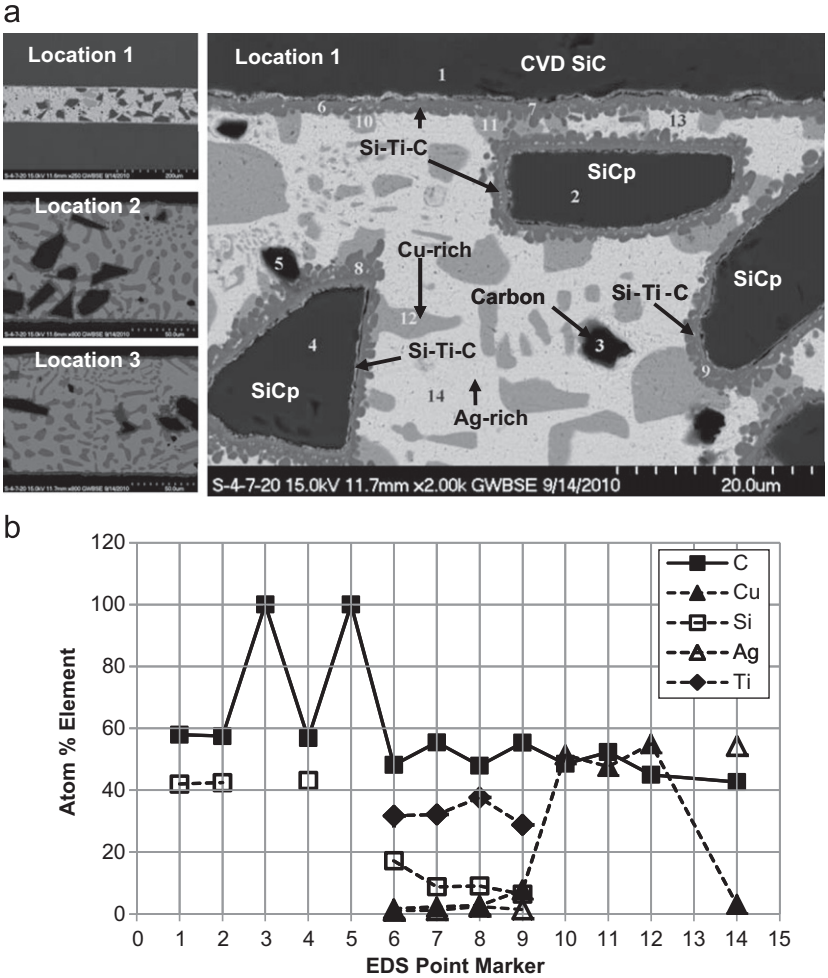

Fig. 4. (a) SEM BSE images of different locations of a CVD SiC/Ticusil/CVD SiC joint with 15 wt% SiC particulates, and a higher magnification view of the joint; (b) relative atomic percentages of the alloying elements at point markers in (a).

forms a contact angle of 85° on stoichiometric TiC and the angle decreases with increasing carbon deficiency in TiCx (i.e. with increasing metallic character of the carbide) ultimately reaching an angle of ~20° at $x=0.5$ [21]. As the interfacial carbide could be sub-stoichiometric, precipitation of Cu would be possible. Additionally, Si enrichment of the interface suggests that besides TiCx, titanium silicides might form at the interface. Titanium silicide has a strong metallic character and is readily wetted by Ag, Cu and Ag–Cu alloys [21] and this also points toward precipitation of Cu-rich phase at the reaction layer. One other possibility may be considered: the presence of SiCp in Cu-rich secondary phases could also be due to 'pushing' of SiCp in the last solidifying liquid, a phenomenon commonly observed in cast metal-matrix composites [22]. The crystallization of Ag-rich primary phase will cause excess Cu to be rejected by the solidification front and the pushing of SiCp by solidifying silver will segregate the SiCp within Cu-rich secondary phases as is actually seen (Figs. 3a and 4a).

The Ti and Si enrichment at the SiC interface is in agreement with the formation of titanium silicides and titanium carbides that was reported in [4,7,12]. The formation of TiC and titanium silicides ($TiSi_2$, Ti_5Si_3, $Ti_5Si_3C_x$) is thermodynamically feasible ($\Delta G<0$). Based on ΔG calculations, it is found that $TiSi_2$ and Ti_5Si_3 are less probable than TiC. Titanium silicides could also form during solidification following SiC dissolution in braze and melt saturation with Si. Titanium silicides exhibit strong thermal expansion anisotropy [23] and a relatively thick silicide layer could lead to uneven shrinkage during cooling of the joint and residual stresses that would weaken the joint in spite of good wetting and bonding.

The reaction layer thickness in the joints varied between 1 and 3 μm which is similar to the reaction layer thickness in joints of sintered SiC fiber-bonded ceramics brazed with Cusil-ABA [24] and comparable to the reaction layer thickness (~2.2 μm) observed by Hanson et al. [25] for unreinforced SiC/Ticusil/SiC joints brazed at 950 °C for 30 min. SEM images of the joints (Figs. 2–4) show that loss of Ti in reaction with SiC particulates has not affected the thickness of the reaction layer on the SiC substrate in the SiCp concentration range (0–15 wt%) and SiCp size (20–30 μm) used in the present study. This general lack of measureable effect of the stated window of time and temperature on reaction layer thickness indicates that initially the reaction kinetics are rapid so that the reaction layer formed at short times changes its thickness only marginally at long times when diffusion controls the growth of the reaction layer and the latter acts as a diffusion barrier inhibiting further growth. The absence of any measureable decrease in reaction layer thickness upon increasing the SiCp content in the present work could be due to a relatively small change in the ceramic's interfacial area because of the coarse SiCp size (20–30 μm) used. In contrast, Hanson et al. [25] noted a significant decrease in reaction layer thickness from ~2.2 μm in the unreinforced Ticusil braze to ~0.6 to 0.9 μm at 5 vol% SiC in Ticusil; the larger interfacial area with the finer size (1–7 μm) SiCp used by them led to a measureable thinning

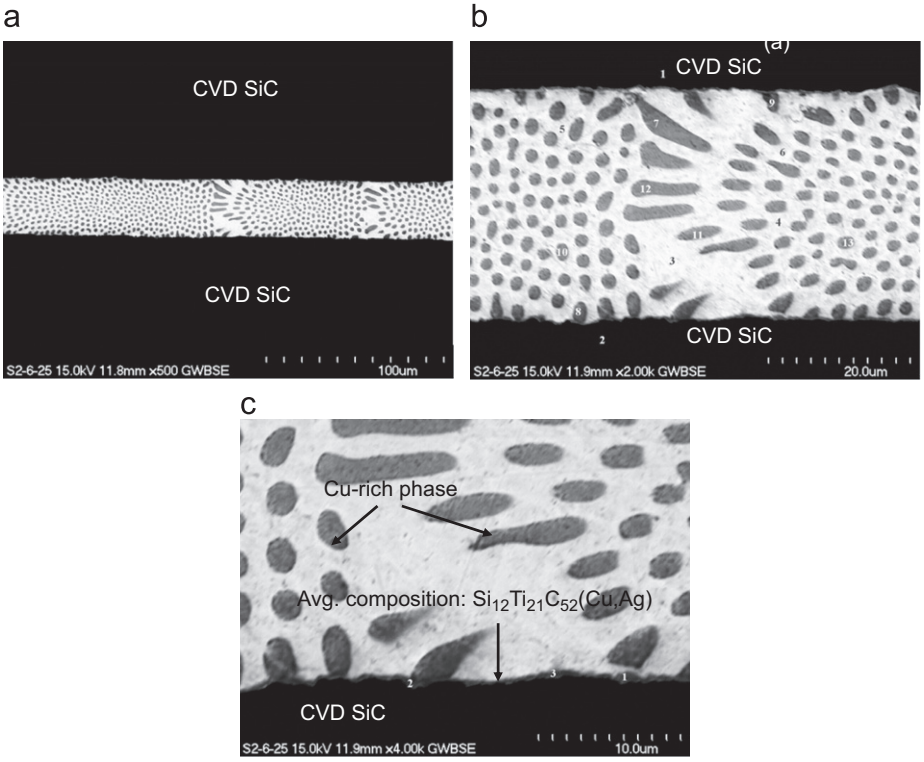

Fig. 5. (a)–(c) SEM BSE images at different magnifications of a CVD SiC/Cusil-ABA/CVD SiC joint with 0 wt% SiC particulates.

of the reaction layer. However, subsequent decrease in reaction layer thickness upon increasing the SiCp content from 5% to 20% was marginal [25]. Both very thick and very thin reaction layers adversely affect the joint strength; very thick layers cause excessive brittleness and very thin layers provide insufficient interfacial strengthening.

The lower magnification views in Figs. 2–4 show that there was no segregation or clustering of SiCp even at a concentration of 15 wt% (43 vol%). Because of the relatively large SiCp size, there is neither crowding nor particle-to-particle contact. Additionally, in spite of a large difference in the densities of SiCp and Ticusil (ρ_{SiC}: 3210 kg m^{-3} and ρ_{braze}: 9400–9800 kg m^{-3}), there was no evidence of segregation from buoyancy-driven floatation in quiescent molten braze. This is due to the wall effect within the narrow braze layer which restricted movement because of the large ratio of SiC diameter-to-braze thickness.

3.2. Microstructure of Cusil-ABA Joints

Figs. 5–8 show SEM backscattered electron (BSE) photomicrographs of SiC/SiC joints made using Cusil-ABA braze reinforced with 0, 5, 10 and 15 wt% SiCp. In spite of overall microstructural similarity (e.g., eutectic structure with Cu-rich and Ag-rich phases) of joints made using Ticusil and Cusil-ABA brazes with 0% SiCp (Figs. 1 and 5), there is a marked difference in the joint microstructures: Cusil-ABA matrix (Fig. 5b) does not have plate-like precipitates of a Si–Ti–C-rich phase that was observed in Ticusil matrix (Fig. 1a) with 0% SiCp. This presumably is because on a weight basis, Cusil-ABA (1.75 wt% Ti) contains 61% less titanium than Ticusil (4.5 wt% Ti). As Ti segregates at the interface and reacts with SiC, its concentration in Cusil-ABA matrix decreases even further with the result that Si released from the dissolution of SiC cannot form Si-Ti intermetallics upon

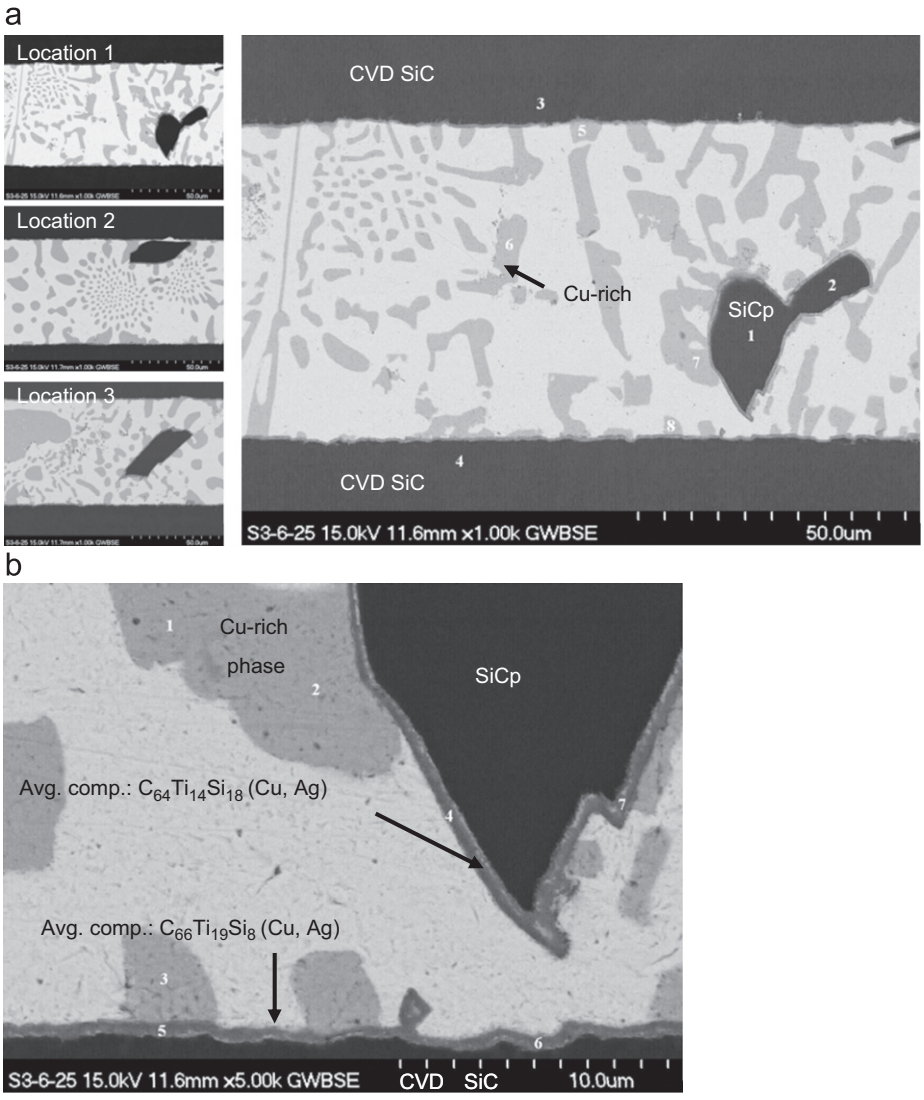

Fig. 6. (a) SEM BSE images of different locations of a CVD SiC/Cusil-ABA/CVD SiC joint with 5 wt% SiC particulates, and (b) a higher magnification view of the SiCp and SiC substrate interfaces with Cusil-ABA.

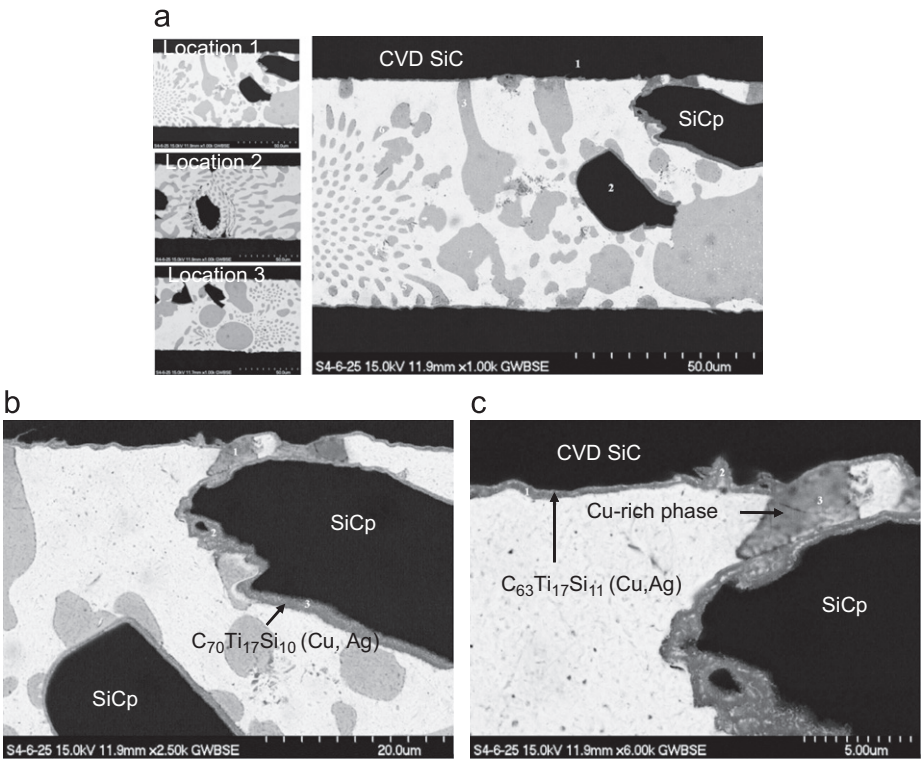

Fig. 7. SEM BSE images of (a) different locations of a CVD SiC/Cusil-ABA/CVD SiC joint with 10 wt% SiC particulates, and (b) & (c) higher magnification views of the SiCp/Cusil-ABA interface and SiC substrate/Cusil-ABA interface.

cooling and solidification. The CVD SiC/Cusil-ABA interface is enriched in Ti, Si and C (Fig. 5c). No differences in the microstructure of the joints made using braze foil and braze paste were noted.

In the case of joints made using SiCp-reinforced Cusil-ABA braze, the distribution of SiCp in Cusil-ABA is random and the reacted SiCp/braze interface and CVD SiC/braze interface serve as sites for precipitation of Cu-rich secondary phases (Figs. 6–8) in a manner similar to the Ticusil joints. The reaction layer thickness on SiCp and CVD SiC substrate in Cusil-ABA joints is smaller than the reaction layer thickness at corresponding interfaces in Ticusil joints. This correlates with the smaller Ti content and the lower brazing temperature of Cusil-ABA than Ticusil; both factors will lead to a less intense interfacial reaction with SiC and a smaller reaction layer thickness.

3.3. Hardness and residual stress

Fig. 9 and Tables 2 and 3 present the hardness data for the CVD SiC/SiC joints made using Ticusil (Fig. 9a) and Cusil-ABA (Fig. 9b). Considering that Knoop values are sensitive to the local variations in the microstructure along the indenter's path, the hardness traces for each type of joint can be considered to be reproducible. On an average, the hardness distributions obtained in joints made using braze foil and braze paste were similar for both Ticusil and Cusil-ABA joints. The measured hardness of the CVD SiC substrate is quite reproducible with an average value of 3279.8 HK (for the SiC substrate in Ticusil joints) and 3298.3 HK (for the SiC substrate in Cusil-ABA joints); the Knoop hardness of CVD SiC is reported in the literature to be in the range 2460–2800 HK. The hardness drops precipitously over the narrow braze region (Fig. 9a and b). Fig. 9 and Tables 2 and 3 show that SiC particulate dispersions lower the hardness of the braze matrix in both Ticusil and Cusil-ABA brazes. The effect on hardness of adding SiCp reinforcement to braze matrix is initially more pronounced for Ticusil than Cusil-ABA at small SiC contents. For example, the hardness for Ticusil drops from 252 HK for the unreinforced braze to 86 HK with 5 wt% SiC and the corresponding drop for Cusil-ABA is from 128 HK to 81 HK. At higher percentages of SiC additions, the hardness values roughly stabilize although Cusil-ABA at 15% SiC shows somewhat higher hardness (avg. value: 147.8 HK) than Ticusil (avg. value: 105.8 HK). The initial drop in HK at 5% is a result of the loss of Ti in interfacial reactions at increased surface area of the ceramic (substrate plus particulates). As Ti is scavenged out of the Ag–Cu–Ti braze and used up in interfacial reactions, its concentration in the braze matrix decreases and lowers braze hardness. A decrease in hardness (and strength) of braze from Ti depletion will be offset by the reinforcing effect of hard SiC particulates. In addition, incorporation of any excess titanium added to the braze shall compensate for the loss of Ti in interfacial reactions leading to high shear strength in joints [12]. Excessive addition of SiC particles [12], however, is known to cause clustering, metal-starved cavities, pores, and sites for crack initiation; all of which lower the joint strength at high particulate loading.

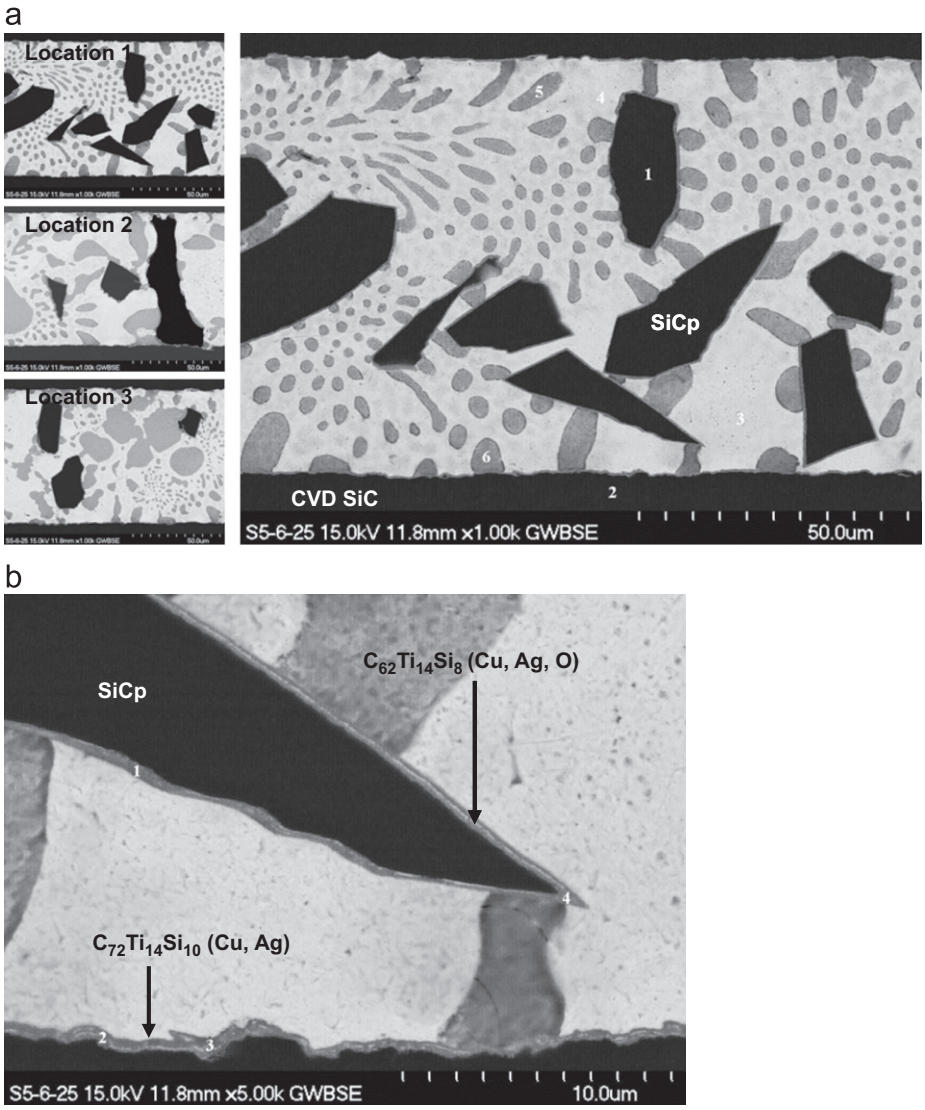

Fig. 8. SEM BSE images of (a) different locations of a CVD SiC/Cusil-ABA/CVD SiC joint with 15 wt% SiC particulates, and (b) a higher magnification view of the SiCp/Cusil-ABA interface and SiC substrate/Cusil-ABA interface.

Degradation of material properties upon loss of key alloy constituents in interfacial reactions has been observed in a number of systems [22]. For example, in metal-matrix composites such as Al–Mg matrix alloys reinforced with aluminosilicate fibers, loss of Mg in interfacial reactions that formed oxide (MgO) and spinel ($MgAl_2O_4$) compounds impaired the age-hardening response of the composite. This has been overcome by either limiting the deleterious reactions via diffusion coatings or adding excess Mg to the matrix alloy to make up for the loss in interfacial reactions. In the present brazed ceramic systems, it would be interesting to separate the effects of strengthening achieved via high Ti additions and strengthening from the SiC particulates without excess Ti additions. In order to separate these effects no excess Ti was added to the braze matrix in the present study.

The primary reasons for adding SiCp to braze alloys was to control the CTE and strengthen the braze matrix. The mismatch of CTE is a critical factor in forming integral joints particularly ceramic–metal joints where CTE mismatch is usually very large. The magnitude of residual stresses arising from the CTE mismatch may be estimated using simplified calculations. For a planar joint configuration between two elastic solids, the residual stress at the interface after brazing under plane-stress condition can be estimated from, $\sigma = (E_c/2)\Delta T \Delta\alpha$, where ΔT is the temperature range, and $\Delta\alpha$ is the difference in the linear CTE values. The stress at the interface in the metal is obtained by taking $\Delta\alpha = (\alpha_m - \alpha_c)$ and the stress in the ceramic is equal but opposite i.e., with $\Delta\alpha = (\alpha_c - \alpha_m)$ in the preceding equation. For the SiC/Ticusil joint using generic property data for SiC ($E = 468$ GPa, $\alpha_c = 4.1 \times 10^{-6}\ K^{-1}$) and with $\Delta T \sim 883$ °C, the residual stress in SiC directly bonded to Ticusil (assumed to be elastic) is about 2.98 GPa. This value exceeds the fracture strength of SiC (~400–575 MPa) indicating failure in the SiC substrate. This simple calculation ignores the deformation of the ductile filler metal and the three-dimensional state of stress in the

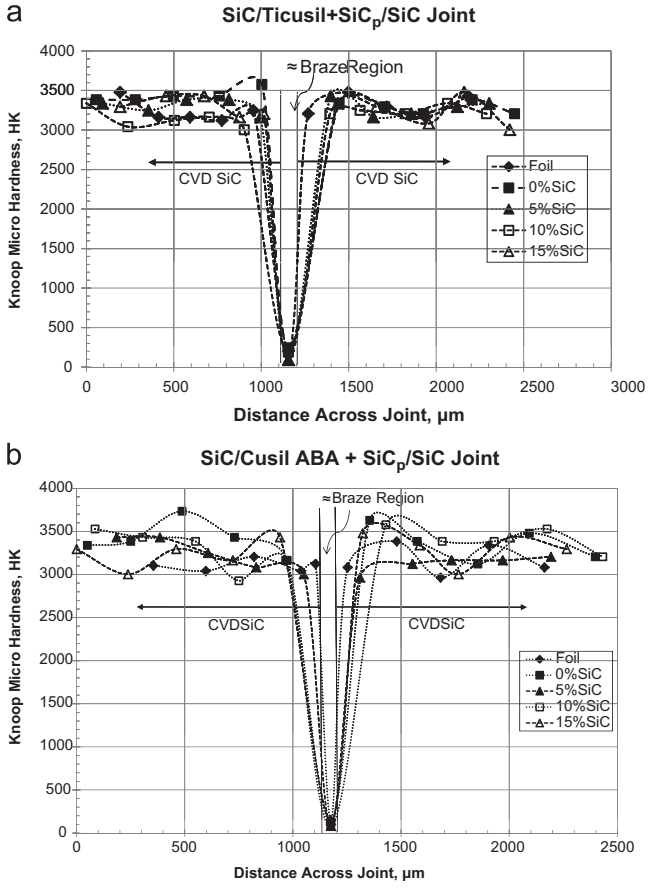

Fig. 9. Knoop microhardness profiles across CVD SiC/SiC joints with different percentages of SiC particulates for (a) Ticusil and (b) Cusil-ABA braze. Also shown are hardness profiles for CVD SiC/SiC joints made using unreinforced braze foil.

Table 2
Mean (μ) and standard deviation (σ) HK of Ticusil joints.

	Ticusil paste							
	0 wt% SiCp		**5 wt% SiCp**		**10 wt% SiCp**		**15 wt% SiCp**	
	μ	σ	μ	σ	μ	σ	μ	σ
CVD SiC	3441.6	71.4	3303.8	85.5	3133.8	116.9	3305.2	119.3
Braze	251.8	57.8	86.0	4.9	116.9	51.7	105.8	31.2
CVD SiC	3285.6	71.0	3286.6	94.9	3241.0	51.3	3239.2	111.0

joint but it highlights the very large residual stresses that develop in directly bonded ceramic–metal joints.

To an extent, residual stresses due to temperature excursions can be managed by controlling the CTE. A decrease in the effective CTE of the composite braze from SiC dispersions can, therefore, be beneficial. Projections of the effect of SiC content on the CTE of the composite braze can be made using models due to Kerner [26] and Turner [27] both of which apply to discontinuous (e.g., particulate-reinforced) two-phase composites with a continuous matrix. Denoting volumetric CTE by β, the effective CTE of the composite braze containing spherical

Table 3
Mean (μ) and standard deviation (σ) HK of Cusil-ABA joints.

	Cusil-ABA paste							
	0 wt% SiCp		**5 wt% SiCp**		**10 wt% SiCp**		**15 wt% SiCp**	
	μ	σ	μ	σ	μ	σ	μ	σ
CVD SiC	3410.2	185.4	3239.2	175.6	3286.8	215.8	3237.2	144.4
Braze	127.7	3.3	80.9	7.7	74.9	11.3	147.8	67.0
CVD SiC	3364	183.0	3124	84.3	3416	130.3	3309	166.4

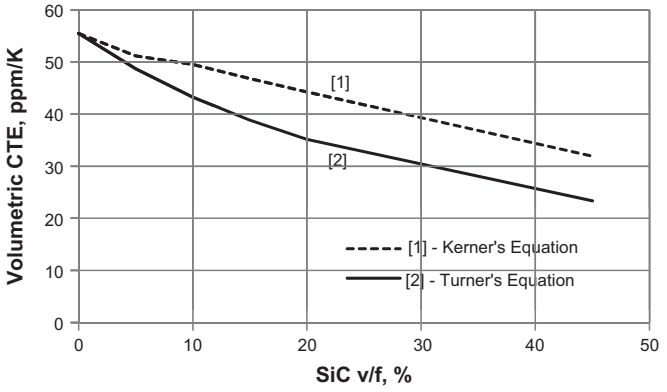

Fig. 10. Projections of the effect of SiC reinforcement on the volumetric CTE of Ticusil (or Cusil-ABA) braze on the basis of Kerner's equation [26] and Turner's equation [27].

particles can be calculated using Kerner's equation [26]. The equation is:

$$\beta_C = \beta_m V_m + \beta_p V_p - (\beta_m - \beta_p) V_m V_p \left[\frac{(1/K_m) - (1/K_p)}{(V_m/K_p) + (V_p/K_m) + (3/4G_m)} \right] \quad (1)$$

where β_c is the volumetric CTE of composite, β_m the volumetric CTE of matrix, β_p=volumetric CTE of particulate, V_m the volume fraction of matrix, V_p the volume fraction of particulate K_m=bulk modulus of matrix, K_p=bulk modulus of particulate and G_m the Shear modulus of matrix. Here $\beta_m = 55.5 \times 10^{-6}\,K^{-1}$, $\beta_p = 12.3 \times 10^{-6}\,K^{-1}$, $E_m = 85$ GPa, $\nu \sim 0.25$, and $K_p = 203$ GPa. The shear modulus and bulk modulus of the composite braze were obtained from the following relationships: $G_m \sim 0.4E = 34$ GPa, and $K_m = E/[3(1-2\nu)] = 57$ GPa. When thermal shear stresses are low, an equation due to Turner [27], given below, is used to predict the volumetric CTE

$$\beta_c = \frac{\beta_m V_m K_m + \beta_p V_p K_p}{V_m K_m + V_p K_p} \quad (2)$$

Fig. 10 shows the dependence of composite CTE on SiC content based on Kerner and Turner equations. At 15 wt% (43 vol%) SiC in Ticusil, the volumetric CTE is projected to decrease by 45% (Kerner's equation) to

60% (Turner's equation), indicating the possibility of stress accommodation in joints via dual effects of decreased CTE and decreased braze hardness (increased ductility) that was observed in the present study. The Kerner and Turner models are known to provide the upper and lower bounds, respectively, on effective CTE, and cover most of the experimental measurements on CTE of ceramic–metal composites [28]. This should validate the estimates of the CTE of composite SiCp–Ticusil and SiCp–Cusil-ABA brazes. The estimates for the CTE of SiCp reinforced Cusil-ABA are nearly identical with those for the reinforced Ticusil braze. This is because the CTE values of the two unreinforced brazes (Table 1) are identical and the SiCp volume fractions differ by less than a percent between Ticusil and Cusil-ABA their densities being 9400 and 9800 $kg\,m^{-3}$, respectively, per the manufacturer.

What emerges from the above discussion is the fact that significantly larger volume fractions (~43%) of coarse SiC particles can be incorporated in the braze than fine SiC (~1–7 μm [12]) thus enabling residual stress management in joints with a considerably reduced CTE. Attempts to incorporate such large (~40–50%) volume fractions of fine SiCp in braze using conventional powder mixing technologies invariably leads to inhomogenous distribution and deleterious flaws, and is not recommended. Although large (~45–55%) reinforcement loadings are readily achieved in pressure-infiltrated metal–matrix composites, the method is not suitable for making particulate-reinforced brazes for use in narrow gaps. In ceramic/ceramic joints but especially in ceramic/metal joints in which ductile interlayers play a critical role in preventing the fracture of the ceramic from residual stresses, the dispersion of hard SiCp shall partially mitigate the stresses by reducing the CTE. The loss in braze ductility and toughness from hard particle dispersions shall be partially compensated by a decrease in braze hardness (increase in ductility and toughness) resulting from Ti-scavenging interfacial reactions.

4. Conclusions

Two Ag–Cu–Ti braze alloys, Ticusil and Cusil-ABA, reinforced with 5, 10 and 15 wt% SiC particulates were used to join CVD silicon carbide to itself to control braze thermal expansion to mitigate residual stresses, and to enhance the joint strength. The reinforcement particles randomly distributed in the braze matrix and bonded to it via reaction with the titanium of the braze, that led to segregation of Ti, Si and C at the SiCp/braze interface. The Si–Ti–C-rich reaction layers (~1–3 μm) facilitated precipitation of the Cu-rich secondary phase on SiCp surface. The Si–Ti–C-rich reaction layers also formed at the interface between CVD SiC substrate and the braze alloy. The loss of Ti in reactions with the SiC particulates did not degrade either the joint integrity or the thickness of the reaction layer formed on the CVD SiC substrate. The dispersed SiC particulates lowered the braze hardness by depleting the braze matrix of Ti. With 43 vol% SiCp in Ticusil (or Cusil-ABA), the CTE of the braze is projected to decrease by nearly 45–60%. It is proposed that loss in braze ductility due to dispersion of hard SiC particulates in braze and a loss in the ability of the reinforced braze to accommodate thermal stresses may be compensated by a decrease in the coefficient of thermal expansion (CTE) of the reinforced braze.

Acknowledgment

B.P. Coddington and R. Asthana acknowledge the research support received from the NASA Glenn Research Center, Cleveland, OH.

References

[1] R.S. Okojie, R. Tacina, C. Wey, C. Blaha, Micro Fabrication of SiC Mesoscale Lean Direct Injector Array: Toward Active Combustion Control, Solid-State Sensors, Actuators and Microsystems Conference, TRANSDUCERS 2007 International, Lyon, France, June 10–14, 2007.

[2] R. Tacina, C. Wey, P. Laing, A. Mansour, A Low Lean Direct Injection, Multipoint Integrated Module Combustor Concept For Advanced Aircraft Gas Turbines, NASA/TM-2002-211347, April 2002.

[3] B.P. Coddington, R. Asthana, M.C. Halbig, M. Singh, Active metal brazing and characterization of brazed joints between SiC and metallic systems, in: T. Ohji, M. Singh (Eds.), Ceramic Engineering and Science Proceedings, vol. 31, Wiley, 2010, pp. 151–161.

[4] J.A. Fernie, R.A.L. Drew, K.M. Knowles, Joining of engineering ceramics, International Materials Reviews 54 (5) (2009) 283–331.

[5] M.R. Locatelli, A.P. Tomsia, K. Nakashima, B.J. Dalgleish, A.M. Glaser, New strategies for joining ceramics for high-temperature applications, Key Engineering Materials 111–112 (1995) 157–190.

[6] P. Prakash, T. Mohandas, P.D. Raju, Microstructural characterization of SiC ceramic and SiC–metal active metal brazed joints, Scripta Materialia 52 (2005) 1169–1173.

[7] Y. Liu, Z.R. Huang, X.L. Liu, Joining of sintered SiC using AgCuTi active brazing alloy, Ceramics International 25 (8) (2009) 3479–3484.

[8] J.V. Marzik, T. Oyama, W.J. Moberly Chan, W.F. Croft, Characterization of a ceramic–metal-ceramic bond: chemical vapor deposited (CVD) silicon carbide joined by a silver-based active brazing alloy, in: S.E. Saddow, D.J. Larkin, N.S. Saks, A. Schoener (Eds.), Silicon Carbide 2002-Materials, Processing and Devices, vol. 742, MRS Proceedings (Symposium K), MRS, Boston, MA, 2002.

[9] V. Trehan, J.E. Indacochea, M. Singh, E. Lugscheider, I. Buschke, Silicon carbide brazing and joint characterization, Journal of Mechanical Behavior of Biomedical Materials 10 (5–6) (1999) 341–352.

[10] J.E. Indacochea, Z. Zhou, M. Singh, Advances in brazing and soldering technologies, in: P.T. Vianco, M. Singh (Eds.), American Welding Society and ASM International, , 2000, pp. 330–337.

[11] J.R. McDermid, M.D. Pugh, R.A.L. Drew, The interaction of reaction-bonded silicon carbide and Inconel 600 with a nickel-based brazing alloy, Metallurgical and Materials Transactions A20 (9) (1989) 1803–1810.

[12] K.M. Knowles, D.R. Ormston, D.B. Conquest, L.J. Ecclestone, J.A. Fernie, Particulate loading of high temperature brazes for joining engineering ceramics, Ceramic Transactions 138 (2002) 103–119.

[13] G. Blugan, J. Kuebler, V. Bissig, J. Janczak-Rusch, Brazing of silicon nitride ceramic composite to steel using SiC-particle reinforced active brazing allo', Ceramics International 33 (2007) 1033–1039.
[14] M. Galli, J. Botsis, J. Janczak-Rusch, Relief of the residual stresses in ceramic–metal joints by a layered braze structure, Advanced Engineering Materials 8 (2006) 197–201.
[15] G. Lin, J. Huang, H. Zhang, Joints of carbon fiber-reinforced SiC composites to Ti-alloy brazed by Ag–Cu–Ti short carbon fibers, Journal of Materials Processing Technology 189 (2007) 256–261.
[16] Z.P. Wang, J.H. Huang, H. Zhang, X.K. Zhao, Reactive composite brazing of C_f-SiC composites to Ti alloy with (Ag–6Al)+Ti+C composite filler materials, Materials Science And Technology 27 (1) (2011) 49–52.
[17] Y. Qin, Z. Yu, Joining of C/C composite to TC4 using SiC particle-reinforced brazing alloy, Materials Characterization 61 (2010) 635–639.
[18] M.C. Halbig, M. Singh, H. Tsuda, Integration technologies for silicon carbide-based ceramics for micro-electro-mechanical system lean direct (fuel) injector application, International Journal of Applied Ceramic Technology 9 (4) (2012) 677–687.
[19] M. Singh, R. Asthana, F.M. Varela, J. Martinez-Rodriguez, Microstructural and mechanical evaluation of a Cu-base active braze alloy to join silicon nitride ceramics, Journal of the European Ceramic Society 31 (2011) 1309–1316.
[20] M. Singh, J. Martínez Fernández, R. Asthana, J.Ramirez Rico, Interfacial characterization of silicon nitride/silicon nitride joints brazed using Cu-base active metal interlayers, Ceramics International 38 (4) (2012) 2793–2802.
[21] D.M. Jacobson, D. Humpston, Principles of Brazing, ASM International, Materials Park, OH, 2005, p. 226.
[22] R. Asthana, Solidification Processing of Reinforced Metals, Trans Tech, Switzerland, 1998.
[23] M.C. Halbig, M. Singh, Development and characterization of bonding and integration technologies for fabricating silicon carbide based injector components, in: T. Ohji, M. Singh (Eds.), Ceramic Engineering and Science Proceedings, Wiley, 2009, pp. 1–14.
[24] T. Matsunaga, H.T. Lin, T. Ishikawa, S. Kajii, R. Asthana, M. Singh, Microstructure and mechanical properties of joints in sintered SiC fiber-bonded ceramics, Key Engineering Materials 484 (2011) 9–14.
[25] W.B. Hanson, J.A. Fernie, K.I. Ironside, D.R. Ormston, K.M. Knowles, Active metal brazing: the role of the braze alloy, in: M. Singh, J.E. Indacochea, J.N. DuPont, L. Ikeuchi, J. Martinez-Fernandez (Eds.), Joining of Advanced and Specialty Materials II, ASM International, Materials Park, OH, 2000, pp. 53–57.
[26] E.H. Kerner, The elastic and thermo-elastic properties of composite media, Proceedings of the Physical Society B69 (1956) 808–813.
[27] P.S. Turner, Thermal-expansion stresses in reinforced plastics, Journal of Research of the National Bureau of Standards 37 (1946) 239–260.
[28] C.L. Hsieh, W.H. Tuan, Thermal expansion behavior of a model ceramic–metal composite, Materials Science and Engineering A 460–461 (2007) 453–458.